Electronic Supplementary Information for Dalton Transactions

Dissymmetry of an Exogenous Bridging Ligand Facilitates the Assembly of a Ferromagnetic and Chiral [$Ni^{II}Cu^{II}$] Complex

Alok Ranjan Paital,[a] Joan Ribas,[b] Leoní A. Barrios,[b] Guillem Aromí*[b] and Debashis Ray*[a]

[a] *Department of Chemistry, Indian Institute of Technology, Kharagpur 721 302, India. Fax: 91-3222-82252; Tel: 03222-283324; E-mail: dray@chem.iitkgp.ernet.in*

[b] *Departament de Química Inorgànica, Universitat de Barcelona, Diagonal, 647 08028-Barcelona, Spain. Fax: +34 93 490 7725; Tel: +34 93 402 1271; E-mail: guillem.aromi@qi.ub.es*

Materials and Physical Measurements. The chemicals used were obtained from the following sources: Triethylenetetramine from S.D. Fine Chem (India). 2-Formyl phenol from SRL (India). $Ni(OAc)_2{\cdot}4H_2O$ and $Cu_2(OAc)_4{\cdot}2H_2O$ from Spectrochem (India). All other chemicals and solvents were reagent grade materials and were used as received without further purification. The elemental analyses (C, H, N) were performed with a Perkin-Elmer model 240 C elemental analyzer. IR spectra were recorded on a Perkin-Elmer 883 spectrophotometer. The solution electrical conductivity and electronic spectra were obtained using a Unitech type U131C digital conductivity meter with a solute concentration of about 10^{-3} *M* and a Shimadzu UV 3100 UV-vis-NIR spectrophotometer respectively. The room temperature magnetic susceptibilities in the solid state were measured using a home built Gouy balance fitted with a polytronic d.c. power supply. The experimental magnetic susceptibilities were corrected for the diamagnetic response using Pascal's constants. Magnetic measurements were carried out in the "Servei de Magnetoquímica (Universitat de Barcelona)" on polycrystalline samples (ca. 30 mg) using a Quantum Design MPMS XL-5 SQUID susceptometer operating at a constant magnetic field of 0.5 T between 2 and 300 K. The experimental magnetic moment was corrected for the diamagnetic contribution from the sample holder and the diamagnetic response from the sample, which was evaluated from Pascal's constants. X-Band EPR measurements (9.7857 GHz) were performed at room temperature and ca. 77K on

powdered samples a Bruker Spectrometer (ESR 300E), working with an oxford helium liquid cryostat for variable temperature. Mass Spectrometry measurements were conducted on a LC/MSD TOF spectrometer from Agilent Technologies, allowing the analysis of exact mass measurements by ESI/APCI by direct introduction and coupling of LC/MS.

Crystallographic data of 1. $C_{34}H_{34}CuN_4NiO_6$, M_r = 716.90, orthorhombic, space group $P2_12_12_1$, a = 11.245 Å, b =16.719 Å, c = 16.859 Å, V = 3169.5 Å^3, ρ_{calcd} = 1.502 g /cm^3 and Z = 4. With the use of 3131 unique reflections collected at 293 K with Mo Kα radiation (λ = 0.71073 Å) out to θ range = 1.72 to 24.97 ° on a CAD4 single-crystal X-ray diffractometer, the structure was solved by using the SHELX-97 programme system and refined by full-matrix least squares methods. The refinement converged to final $R1$ = 0.0437, $wR2$ = 0.1004; and GOF = 1.103 with the largest difference peak and hole as 0.433 and –0.472 e Å^{-3} respectively. CCDC 292428. See http://pubs.acs.org for crystallographic data in cif or other electronic format.

Synthesis of the Complex [Cu(μ-L)(μ-fp)Ni]·H_2O (1): To a methanolic solution (50 ml) of $Ni(OAc)_2·4H_2O$ (0.271 g, 1.09 mmol) and $Cu_2(OAc)_4·2H_2O$(0.217 g, 0.54 mmol), 2-formyl phenol was added and refluxed for 15 minutes followed by addition of H_3L (0.5 g, 1.09 mmol) in hot methanol. The mixture was then was stirred under reflux for 1 hr. Then the resulting solution was filtered and kept for slow evaporation. After slow evaporation for 4 days, a greenish crystalline product was obtained (~75 % yield). The solid was isolated, washed with cold methanol, and dried under vacuum over P_4O_{10}. Anal. Calcd for $C_{34}H_{34}CuN_4NiO_6$: M.W. = 716.90. C, 56.96; H, 4.78; N, 7.81. Found: C, 56.82; H, 4.88; N, 7.66 . Molar conductance, Λ_M : (MeCN solution) 8 ohm^{-1} cm^2 mol^{-1}. UV-visible spectrum (CH_3CN): λ_{max} (ε_{max}) 680 (148), 381 (12820). Selected IR bands (KBr, cm^{-1}) 3374w, 1631vs, 1598s, 1531m, 1444m, 1406w, 1334w, 1271w, 1183w, 1149s, 1128w, 900w, 766m.

Table S1. Selected bond lengths (Å) and bond angles(º) for **1**.

O3-Cu1	2.005(5)	O3-Ni1	2.075(5)	O2-Ni1	2.005(5)
O4-Ni1	2.019(5)	O4-Cu1	2.282(5)	O5-Ni1	2.102(6)
Ni1-N4	2.022(6)	Ni1-N3	2.182(5)	Cu1-O1	1.913(5)
Cu1-N1	1.961(6)	Cu1-N2	2.083(6)		

Cu1-O3-Ni1	101.9(2)	Ni1-O4-Cu1	94.72(19)	O2-Ni1-O4	94.8(2)
O2-Ni1-N4	90.4(2)	O4-Ni1-N4	174.8(2)	O2-Ni1-O3	95.04(19)
O4-Ni1-O3	80.70(19)	N4-Ni1-O3	98.3(2)	O2-Ni1-O5	87.4(2)
O4-Ni1-O5	88.0(2)	N4-Ni1-O5	92.8(2)	O3-Ni1-O5	168.6(2)
O2-Ni1-N3	172.8(2)	O4-Ni1-N3	91.9(2)	N4-Ni1-N3	83.0(2)
O3-Ni1-N3	88.69(19)	O5-Ni1-N3	90.15(19)	O1-Cu1-N1	92.0(2)
O1-Cu1-O3	91.7(2)	N1-Cu1-O3	156.7(2)	O1-Cu1-N2	174.7(2)
N1-Cu1-N2	83.0(3)	O3-Cu1-N2	92.1(2)	O1-Cu1-O4	94.9(2)
N1-Cu1-O4	126.4(2)	O3-Cu1-O4	76.09(18)	N2-Cu1-O4	89.6(2)

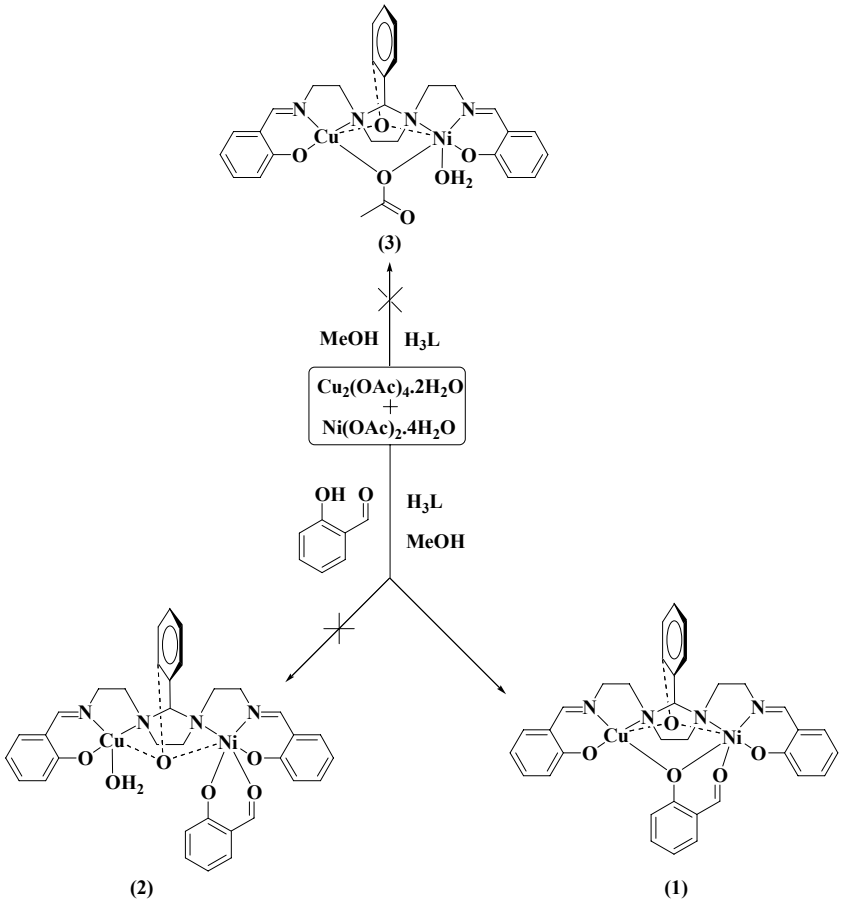

Scheme S1

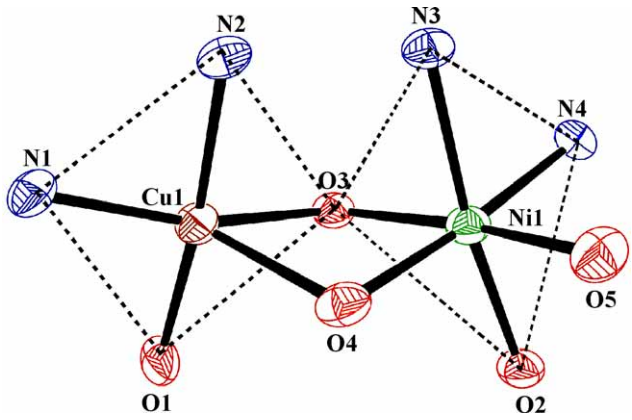

Figure S1. The core structure of complex 1 showing two different geometries of the tetradentate coordination pockets for binding of Cu^{II} and Ni^{II} by L^{3-}.

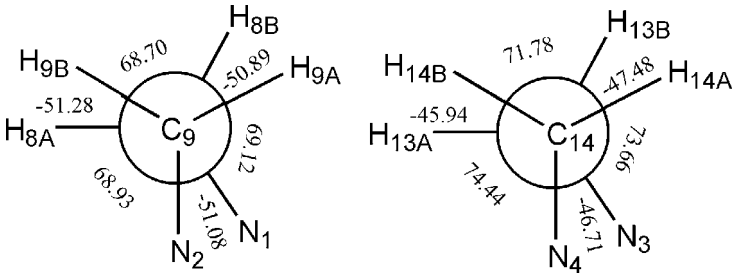

Figure S2. Stereochemistry (*gauche* conformer) of the terminal ethylene arms of the ligand attached to the central imidazolidine ring in **1** as indicated by Newman projections.

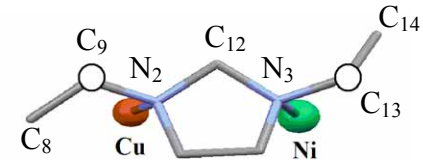

Figure S3. Part of the molecule **1** showing different conformations around the C atoms in α position from the imidazolidine ring (marked as circle).

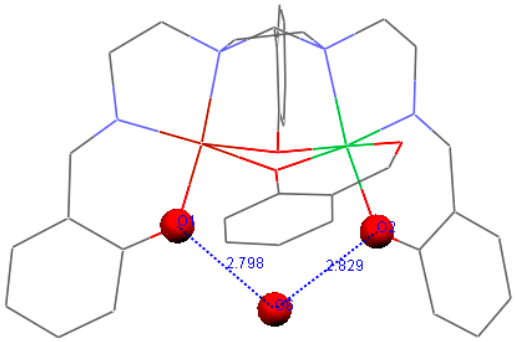

Figure S4. The hydrogen bonding of water molecule of crystallization with terminal coordinated phenolates groups in **1**.

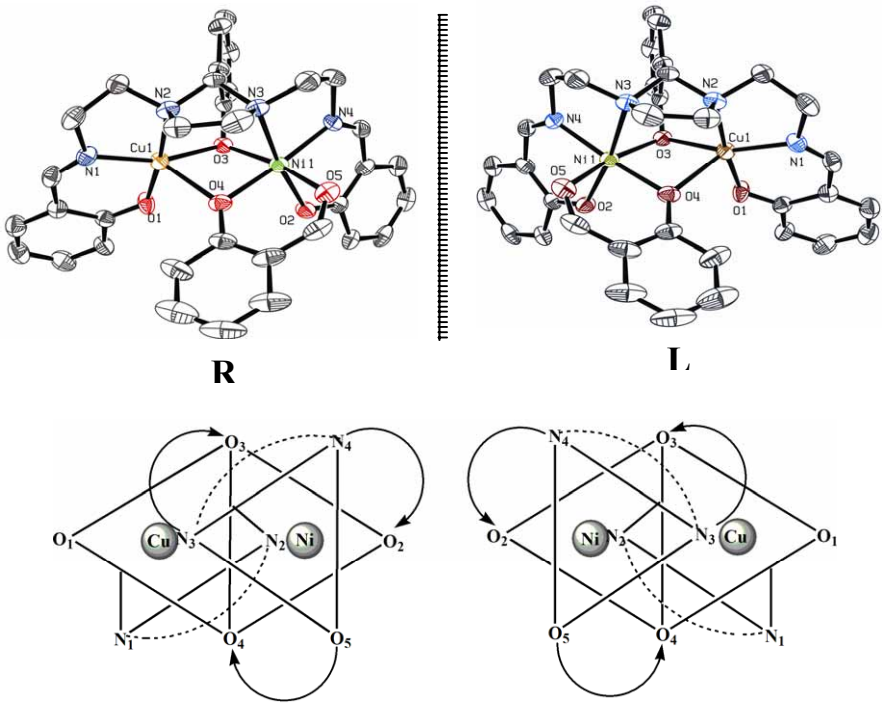

Figure S5. (a) Perspective view of the two enantiomeric forms (R = formyl coordination right, L = formyl coordination left) in complex **1.** O4,O5 = 2-formyl phenolate; O2,N4, N3,O3 = L^{3-}. (b) When viewed through the N3N4O5 trigonal plane of Ni^{II}, the three bidentate chelating arms in R isomer show right (P or Δ) helicity.

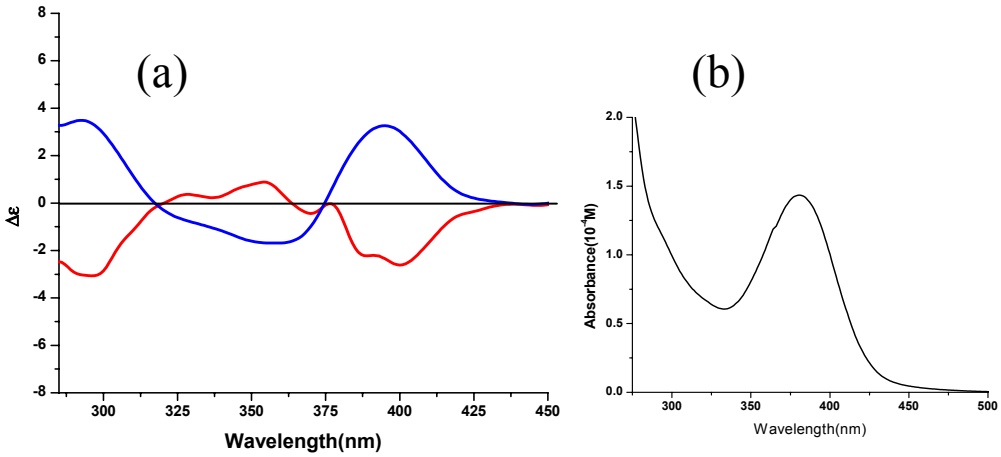

Figure S6. (a) CD spectra of two single crystals of **1** consisting of different enantiomers of the complex, in MeCN solution. (b) UV-vis spectrum of **1** in MeCN solution.

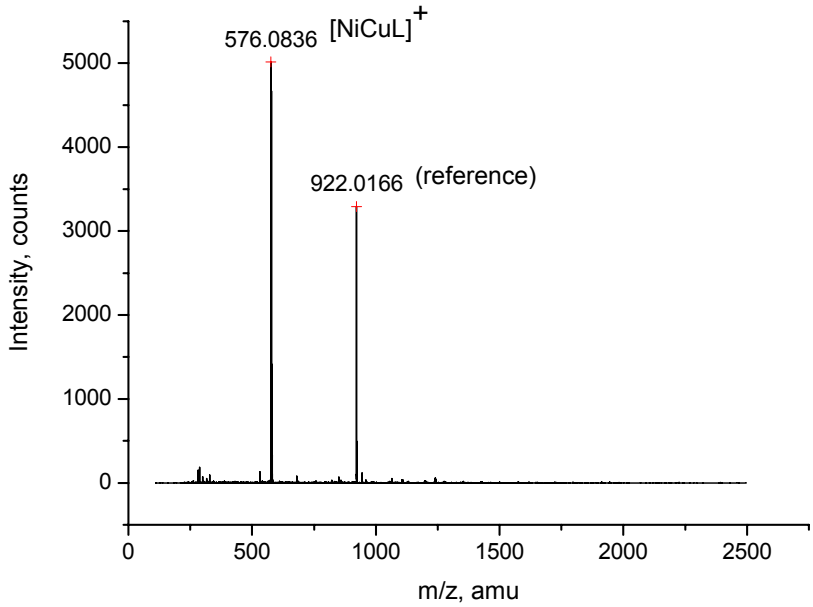

Figure S7. ESI Mass Spectrometry plot of complex **1** in H_2O/MeCN solution (1:1), where only one peak (besides the reference) is observed at $m/z = 576.1$ amu, corresponding to the $[NiCuL]^+$ fragment.

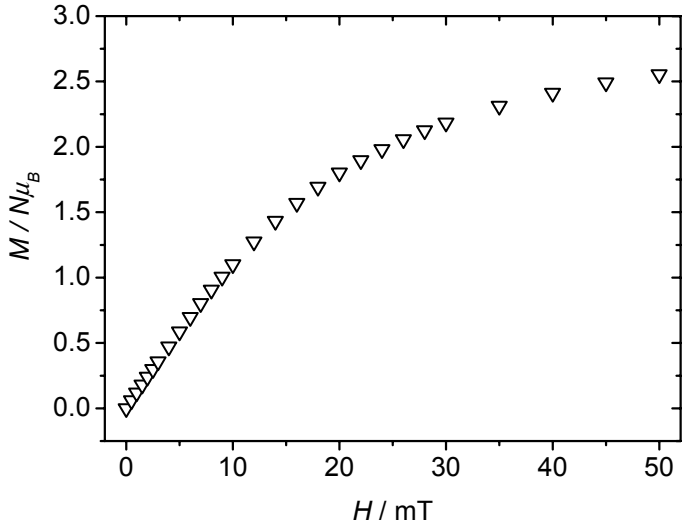

Figure S8. Plot of reduced Magnetization (*M*) *versus* Magnetic Field (*H*) per mol of complex **1** measured at 2K.

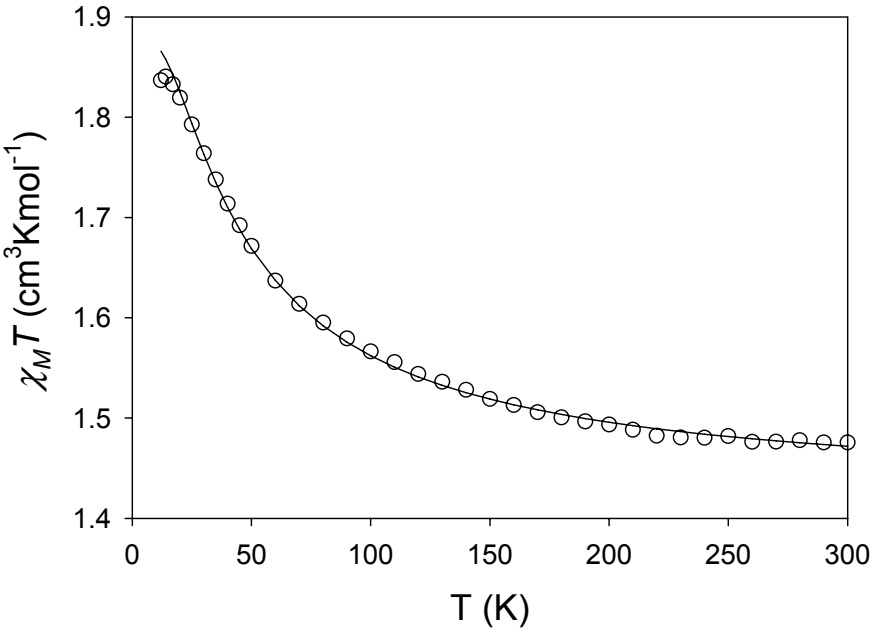

Figure S9. Plot of $\chi_M T$ *vs T versus* T per mol of complex **1** in the 12K to 300K temperature range. The solid line is a fit of these data using the equation

$$\chi_M T = \frac{N\beta^2}{4kT} \times \frac{{g_{1/2}}^2 + 10{g_{1/2}}^2 \exp(6J/2kT)}{1 + 2\exp(6J/2kT)}$$ where; $g_{1/2} = g_{Ni} - \delta$, $g_{3/2} = g_{Ni} + \delta$ and $\delta = (g_{Cu} - g_{Ni})/3$ (see *Inorg. Chem*. **1982**, *21*, 3050-3059)

Here, the same Hamiltonian as in the manuscript was used, without the last term (corresponding to the ZFS). The parameters are J = 11.9 cm^{-1}, $g_{1/2}$ = 2.3 and $g_{3/2}$ = 2.0.

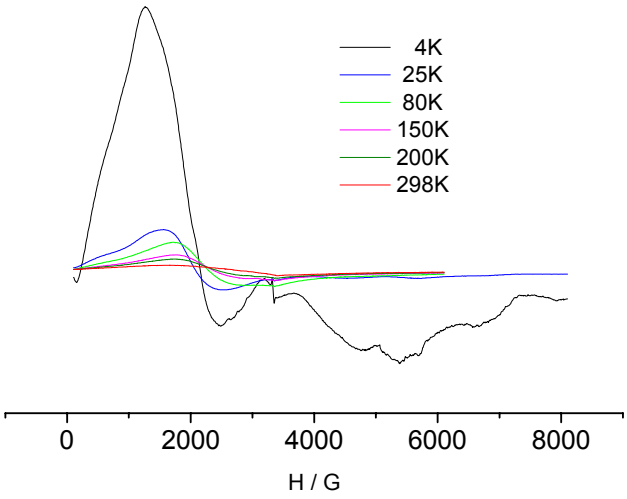

Figure S10. X-band Powder EPR spectra of complex **1** at different temperatures.

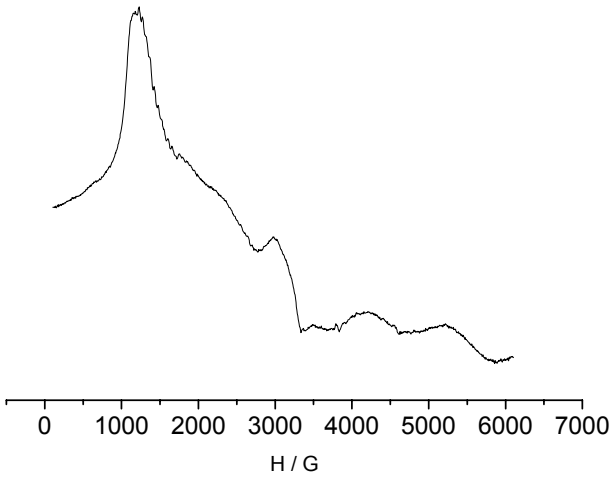

Figure S11. X-band EPR of complex **1** in frozen CH_2Cl_2 solution, at 4 K.